Lightweight locomotion assistant for people

Gonçalo Neves
goncalomneves@tecnico.ulisboa.pt

Instituto Superior Técnico, Lisboa, Portugal

January 2021

Abstract

With the constant increase of the elder population, the number of cases of walking disabilities has grown, together with the need for a less intrusive locomotion aiding device. Most devices developed recently are created with an hospital or clinical use in mind, lacking a device that patients can use at home, while their locomotion disability is still light, or when they finish the heavier hospital attendance like physiotherapy. This paper proposes a robotic cane that gives assistance to people with light locomotion disabilities, helping users maintain and recover their balances in standing and walking situations. The design is based on an unicycle, and is controlled using full-state feedback with gain obtained by LQR and using Polynomial Pole Placement Techniques, with its reference being calculated using the forces applied by the user. The mathematical model, the control and the hardware of the prototype are analysed in detail, and its performance is confirmed by simulations and real-life experiments, verifying its behaviour. The effectiveness of the prototype in real world applications was verified, testing its behaviour when used by users with and without mobility impairments, in situations of normal movement, situations of user standing and situations of danger of imbalance. In all tests, the device performed better than expected, confirming the concept viability.
Keywords: Robotic cane, light locomotion assistance, compact locomotion assistant, locomotion disabilities, unicycle

1. Introduction

The ability to walk upright is one of the most important factors that define an human being. Alongside the massive brain (*homo sapiens*) and the ability to make tools (*homo habilis*), it is one of the distinctive features that separates the human species and its ancestors (*homo erectus*) from the rest of the animals [12]. Alongside that, being able to walk brings not only physical well being to an individual's life but also psychological, social and economic well-being, since that such inability removes a major portion of the patient's freedom and lowers the performance at most activities of daily living [27].

Also, due to low levels of physical strength resulting from muscle weakness or other medical conditions, elderly people are the age group that suffers the most with restricted movement, and, since the elderly population is growing, corresponding to 22.1% of the Portuguese population in 2019, close to 2% higher than the values of 2018 [1], a shortage of young people for nursing care can become a problem [4].

Because of this, walking-aiding means and devices become objects of extreme importance to regenerate the ability to walk to users with conditions that deteriorate or fully remove such capacities without the need of full time evaluation and supervision from nurses, physiotherapist or other professionals.

Studies have been made on Smart Walkers (SWs) for clinical evaluation and assistance of people with decreased locomotion capabilities ([14] [20] [21] [16] [6] [9] [22]). However, these robotized walker devices present a bulky and complicated design that reduces the possibility of its use outside of clinical and hospital environments.

Therefore, a Smart Cane (SC) becomes more adequate for home and individual use, without the constant supervision of medical staff. There are some works made on these types of devices ([15] [23] [3] [26] [25]). This device is more mobile and less intrusive, although it becomes less stable because of the size, structure design and weight. Because of this, it is more appropriate to people that still hold some control over their locomotion, helping to maintain or correcting their gait in order to ensure the conservation of their ability to walk. It can be used also as a second stage for people recovering from ataxic problems or other incorrect gait problems that have already been evaluated and rehabilitated with the help of a Smart Walker (SW) in a clinical environment, being now able to go home with a smaller

and less intrusive device.

Even though these SC's provide a smaller device, most of them are still too big to provide a comfortable use in tighter places and/or require sensors to be connected to the user. The device proposed by this paper has a smaller footprint and requires no sensors connected to the user, presenting a simpler and easier to use application.

2. Background

In order to minimize the footprint that the robot will have, the cane has only one wheel connected to the rod, on which the user grabs Figure 1. With only one moving part, the robot becomes less mechanically complex, the weight is reduced, since it is only needed one motor and one wheel, and, with the reduction of the footprint of the device, the user has more space to move his lower limbs, preventing situations where the user would hit the cane or vice-versa. The wheel used is a simple, traditional wheel, which implies that the cane can only move in two directions, but helps to support of the user, reducing the possibility of the cane to slip sideways, simplifying also the movement of the robot, becoming more predictable for the user.

Figure 1: 3D render of the final vision of the cane

2.1. Model of the Robotic Cane

The model is based on an unicycle, with only one degree of freedom, that consists on the joint between the wheel and the rod, which is where the motor is placed. A simple schematic of the model can be seen in Figure 2.

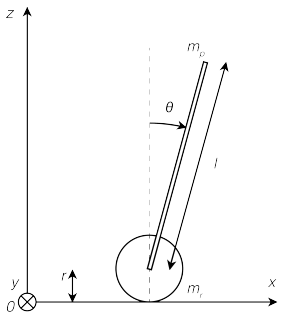

Figure 2: Schematic of the model.

Table 1: Variables of the model.

$\theta[rad]$	angle of the rod
$x[m]$	position of the wheel
$m_p[kg]$	rod mass
$m_r[kg]$	wheel mass
$g[m^2/s]$	gravitational force
$r[m]$	wheel radius
$l[m]$	rod length
$l_c[m]$	length from axle to rod center of mass
$\delta[N \cdot m \cdot s/rad]$	viscous friction coefficient
u	control input (voltage supplied to motors)

Defining a model only with the motor and the rod [5], it is possible to relate the gravitational forces exerted on the rod with the friction and inertia to create a space state model that allows to obtain the angular acceleration of the rod.

The gravitational, friction and inertia components that are applied to the arm can be defined by

$$F_g = \frac{1}{2} m_p g l \sin\theta, \quad F_f = \delta\dot{\theta}, \quad I = \frac{1}{3} m_p l^2 \ddot{\theta}, \quad (1)$$

respectively.

Adding all the components it is possible to obtain the torque that must be applied by the motor to the arm, that is, the system input. As such, the following expression is obtained:

$$u = \frac{1}{3} m_p l^2 \ddot{\theta} + \delta\dot{\theta} + \frac{1}{2} m_p g l \sin\theta. \quad (2)$$

Putting the angular acceleration, $\ddot{\theta}$, in evidence, we obtain the non linear equation of the system:

$$\ddot{\theta} = \frac{u - \frac{1}{2} m_p g l \sin\theta - \delta\dot{\theta}}{\frac{1}{3} m_p l^2}. \quad (3)$$

Adding the wheel to the system, a new variable is added - the position of the wheel. The linear equation of the linear acceleration of the system is obtained by summing the forces acting on the wheel in the horizontal direction,

$$m_c \ddot{x} + N = u, \quad (4)$$

where N is the reaction force that the pendulum exerts on the wheel, and can be obtained through

$$N = m_p \ddot{x} + m_p l \ddot{\theta} \cos\theta - m_p l \dot{\theta}^2 \sin\theta, \quad (5)$$

which corresponds to the sum of the forces acting on the pendulum.

Replacing eq. (5) in eq. (4), we get the second equation of motion in

$$(m_c + m_p)\ddot{x} + m_p l \ddot{\theta} \cos\theta - m_p l \dot{\theta}^2 \sin\theta = u. \quad (6)$$

Due to the fact that the torque generated by the motor not only serves to move the arm but also the wheel, a term has to be added to eq. (2), and the model becomes the linear equations in

$$\begin{aligned}\ddot{x} &= \frac{u - m_p l\ddot{\theta}\cos\theta + m_p l\dot{\theta}^2\sin\theta}{m_r + m_p},\\ \ddot{\theta} &= \frac{(u - \frac{1}{2}\dot{x}m_r r) - \frac{1}{2}m_p g l\sin\theta - \delta\dot{\theta}}{\frac{1}{3}m_p l^2}.\end{aligned} \tag{7}$$

Although x varies widely in values as the unicycle moves, since it represents the position of the wheel, the value of θ is always around zero. This way, it is possible to make the following linearization:

$$\sin\theta \approx \theta,\ \cos\theta \approx 1,\ \dot{\theta}^2 \approx 0, \tag{8}$$

that when applied to (7), originates the following linear equations of motion:

$$\begin{aligned}\ddot{x} &= \frac{u - m_p l\ddot{\theta}}{m_r + m_p},\\ \ddot{\theta} &= \frac{(u - \frac{1}{2}\dot{x}m_r r) - \frac{1}{2}m_p g l\theta - \delta\dot{\theta}}{\frac{1}{3}m_p l^2}.\end{aligned} \tag{9}$$

The linear equations of motion were converted to the traditional model of a state space model,

$$\dot{x} = Ax + Bu, \quad y = Cx + Du. \tag{10}$$

In this specific case, the model after being converted is:

$$\begin{bmatrix}\dot{x}\\ \ddot{x}\\ \dot{\phi}\\ \ddot{\phi}\end{bmatrix} = \begin{bmatrix}0 & 1 & 0 & 0\\ 0 & 0 & 0 & -\frac{m_p l}{m_r+m_p}\\ 0 & 0 & 0 & 1\\ 0 & -\frac{\frac{m_r r}{2}}{\frac{1}{3}m_p l^2} & -\frac{\frac{m_p g l}{2}}{\frac{1}{3}m_p l^2} & -\frac{\delta}{\frac{1}{3}m_p l^2}\end{bmatrix}\begin{bmatrix}x\\ \dot{x}\\ \phi\\ \dot{\phi}\end{bmatrix} + \begin{bmatrix}0\\ \frac{\frac{1}{r}}{m_r+m_p}\\ 0\\ \frac{1}{\frac{1}{3}m_p l^2}\end{bmatrix}u,$$

$$y = \begin{bmatrix}1 & 0 & 0 & 0\\ 0 & 0 & 1 & 0\end{bmatrix}\begin{bmatrix}x\\ \dot{x}\\ \phi\\ \dot{\phi}\end{bmatrix} + \begin{bmatrix}0\\ 0\end{bmatrix}u. \tag{11}$$

The MATLAB ® code of this model can be accessed in [17].

2.2. Control of the Robotic Cane

Using full-state feedback control (eq. (12)), which gain K is obtained by minimizing the quadratic cost function in eq. (13)[10] with MATLAB ®function `lqr()` with parameters $Q = C^T C$ and $R = 0.0001$, the model was simulated for a situation where no forces are applied to the pendulum, only a 10% deviation from the vertical position at the beginning of the simulation. The system's response is represented in Figure 3.

$$u = -KX \tag{12}$$

$$J(u) = \int_0^\infty (x^\intercal Q x + u^\intercal R u + 2x^\intercal N u)dt \tag{13}$$

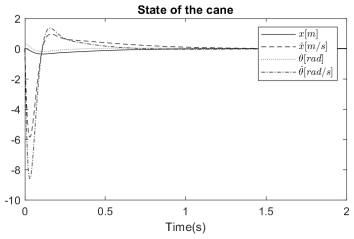

Figure 3: Response of the system to a disturbance, with both references at zero.

In this test the references of both x and θ have been set to zero, just to verify the correct functioning of the model.

However, a reference of zero both in the position of the wheel and in the angle of the cane is not realistic, since these must adapt to the direction and intensity of the forces applied by the user. Thus, a MATLAB ® function was created that obtains a reference for both angle and position. The code can be accessed in [17].

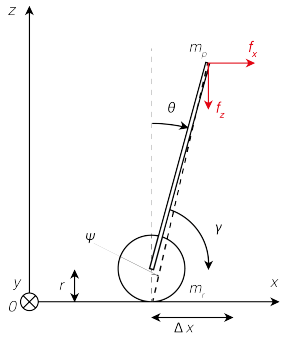

Figure 4: Model schematic with forces applied.

The aim is for the reference to adapt to the force applied by the user. This way, the sum of the forces applied to the pendulum must be zero, that is, the angle of the cane should compensate for the force applied by the user. By analyzing the forces applied to the pendulum, as in Figure 4, it is possible to obtain the following equilibrium equation:

$$-l_c m_p g\sin\theta_{ref} = (l\cos\theta_{ref} + r)f_x + (l\sin\theta_{ref})f_z. \tag{14}$$

Solving eq. (14) for θ_{ref}, the eq. (15) is obtained:

$$\theta_{ref} = \arcsin \frac{\tan\psi}{1+\tan^2(\psi)} \left(\frac{r}{l} + \sqrt{((1 - \frac{r^2}{l^2}) \tan\psi + 1)} \right), \quad (15)$$

, where

$$\tan\psi = \frac{lf_x}{l_c m_p g - lf_z}. \quad (16)$$

Knowing the reference angle θ of the rod it is possible to obtain the angular movement that the wheel should make in relation to the arm through the eq. (17):

$$\gamma_{ref} = \frac{l}{r} \sin\theta_{ref}. \quad (17)$$

By multiplying the angular movement that the wheel should make, γ_{ref}, by the radius of the wheel, the movement that the wheel should make is obtained, which when added to the current position, results in the reference position. Therefore, the reference position can be obtained directly from the reference angle of the arm through eq. (18).

$$x_r = l \sin\theta_{ref} + x. \quad (18)$$

The reference angle and position obtained in (15) and (18), once calculated, are placed in the full-state feedback controller.

In order to verify that the controlled system is able to reach the reference assigned to it, a test was carried out in which a reference of θ with several levels is placed to the system, thus allowing the analysis of the system's behavior when it transits between different angle references while starting with a 10% deviation from the vertical position, as in Figure 3. The result is found in Figure 5.

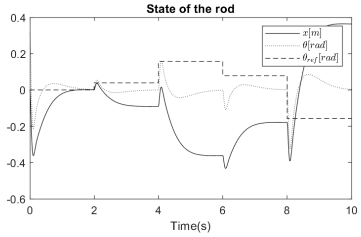

Figure 5: Behaviour of the system to a variable reference.

In all cases the angle of the cane tends to go, initially, to the desired reference, however it does not remain in the reference, sometimes not even reaching it, ending up returning to zero, that is, to the position in which it is stable and in equilibrium. This results from the fact that in simulations the hand of the user, that gives the cane another point of contact other than the floor, is not taken in account (the cane is simulated by itself), and so, the human contribution to the stabilization of the system for references other than is not simulated. In real life testing this behaviour should be corrected.

The system was also simulated being controlled through Polynomial Pole Placement Techniques. The controller has two distinct parts, one controlling the position and another controlling the angle. The (19) angle controller, obtained only through Root-Locus analysis, has two components, each responsible for modifying the poles differently. The first component places the poles of the transfer function of the angle in the left complex semi-plane, making the system stable [19], and the second component adds two poles in the far-left region of the complex plane (negative real component but with high absolute value) making the system causal [11].

$$\begin{aligned} \frac{Y_{ctrl\_ang1}(s)}{X_{ctrl\_ang1}(s)} &= 60\frac{9.375s - 3.2225}{s - 3} \\ \frac{Y_{ctrl\_ang2}(s)}{X_{ctrl\_ang2}(s)} &= \frac{s^2 + 20s + 101}{s^2 + 200s + 10000} \end{aligned} \quad (19)$$

However, due to the complexity of the position component, the respective controller (20) was obtained through polynomial pole placement techniques [7], placing the poles in $\lambda_1, \lambda_2 = -8 \pm j$, $\lambda_3, \lambda_4 = -6 \pm j$, $\lambda_5, \lambda_6 = -2 \pm 0.5j$ and $\lambda_7 = -2,42$, which resulted in only one component,

$$\frac{Y_{ctrl\_pos}(s)}{X_{ctrl\_pos}(s)} = \frac{-2926s^3 - 13024s^2 - 413s - 215.5}{s^3 + 34.19s^2 + 18785s + 78721}. \quad (20)$$

The two parts return two control signals, one each, that are combined by applying a weight to each one, α and $1 - \alpha$, which represent the importance given to the position and angle respectively. The weights used were 21% for the position and 79% for the angle, having been obtained by performing simulations with different weights and comparing the performance of each using the Root Mean Squared Error (RMSE) and observing the behavior of the system, choosing the option that presented the best behavior.

Two force signals were created, simulating the forces an user would apply on the handle, as in Figure 4, when walking slowly (0.25m/s), normally (1m/s) and faster (2m/s), and were used to calculate the reference through eqs. (15) and (18). The system controlled through Polynomial Pole Placement Techniques was then simulated with the references obtained. The response of the system for the slow walking case is shown in Figure 6.

The results show that, compared to the LQR option, the system is able to reach the reference with higher success, at the cost of making the behaviour of the cane less smooth.

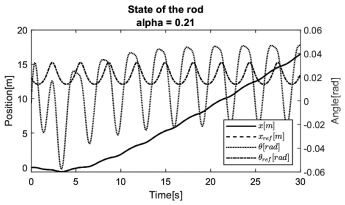

Figure 6: Behaviour of the system controlled by pole placement, in a situation of normal movement (1m/s).

An adaptive control option was also tested, but presented poor results, and so was not implemented.

3. Implementation

3.1. Robot components

The total list of components used is a controller, two motors, a motor driver, an inertial measurement unit (IMU), an encoder, two batteries, a Bluetooth module and two force sensitive resistors. The datasheets of all components can be accessed in [18].

The controller used is an Arduino Uno. In order to obtain the angle of the cane and the position of the wheel, an IMU and an encoder were used. The controller receives data from the sensors and calculates the control signal that it has to send to the motors. As a direct connection between the controller and the motors is not feasible, because not only the output currents of the controller are insufficient for the motors, but the electrical noise generated by the motors can damage the controller, a motor driver had to be used. In the aluminium prototype, a Bluetooth module and two force sensitive resistors were added. The whole prototype is powered by two batteries, separating the power circuits of the motors and the micro-controller. A Kalman filter [10] is used to clean and combine the signals from the gyro and the accelerometer of the IMU, with parameters $Q_{angle} = 0.001$ and $Q_{bias} = 0.003$ corresponding to the process noise variance for the accelerometer and the gyro bias, respectively, and $R_{measure} = 0.03$ corresponding to the measurement noise variance.

3.2. Robot prototype

In total, three prototypes were built. The wiring diagram for all prototypes can be seen in [18]. The average mass that an elderly person (60+ years old) can lift, from the hip to the shoulder, in 4 consecutive repetitions, is $20.2kg$ for men and $13.2kg$ for women [13]. In order to add a comfort gap, reducing the fatigue caused by transporting the cane in situations where it has to be raised repeatedly, a limit of $7kg$ has been placed on the mass it should have, corresponding to approximately half of the lowest value previously mentioned.

In order to verify the viability of the concept, a smaller prototype was built using LEGO ® parts as its structure, to check the correct functioning of the components and the behaviour of the control at a smaller scale. The tests performed with this small prototype showed that although the control and the IMU were working as intended, the encoder wasn't working properly due to flexibility of the LEGO ® structure and lack of robustness of the sensor. Because of this, this sensor was not used in other prototypes.

An aluminum tube was added to the smaller prototype in order to change its size to a more realistic level, while still using the LEGO ® structure. This robot, which can be seen in Figure 7 has the specifications represented in Table 2,

Figure 7: Bigger LEGO ® prototype of the robot.

Table 2: Parameters of the bigger LEGO ® prototype.

rod mass $[kg]$	0.593
wheel mass $[kg]$	0.060
wheel radius $[m]$	0.080
rod length $[m]$	0.875
length from axle to rod center of mass $[m]$	0.190
viscous friction coefficient $[N \cdot m \cdot s/rad]$	0.025

Figure 8: Aluminium prototype of the robot.

The aluminum prototype, represented in Figure 8, was created in order to test the concept with real users without limitations due to the fragility of the robot. The structure is made of aluminum, increasing the integrity and robustness of the robot, while maintaining reduced mass. The complete prototype has a mass just over $800g$, well below the mass limit imposed at the beginning of this chapter. This prototype was equipped with the two force

sensors in the handle, like is shown in Figure 9, and with the Bluetooth module, allowing data to be obtained without a cable connecting the cane to a computer.

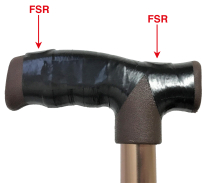

Figure 9: Positioning of force sensors on the handle.

This prototype was presented and tested with a medical team, composed of elements from SPMS (Serviços Partilhados do Ministério da Saúde) and ACES (Agrupamento de Centros de Saúde) Loures-Odivelas, in order to analyze and adjust its behavior and make the necessary changes in order to meet the needs and characteristics of patients with reduced mobility. Due to the small variations that occur in the hands of people in an unconscious way, mainly in old ages where problems like Parkinson's can arise, a band of $\pm 5°$ around the vertical position was implemented of this prototype where the gain of the controller is reduced by 80%, making the use of the cane more comfortable and smooth. The parameters of this prototype can be seen in Table 3

Table 3: Parameters of the aluminum prototype.

rod mass $[kg]$	0.810
wheel mass $[kg]$	0.060
wheel radius $[m]$	0.08
rod length $[m]$	0.780
length from axle to rod center of mass $[m]$	0.20
viscous friction coefficient $[N \cdot m \cdot s/rad]$	0.25

A code was created for the Arduino in order to control the prototypes created. As in MATLAB ® simulations, control is done through full-state feedback (eq. (12)) with gain obtained by LQR and through Polynomial Pole Placement Techniques. All Arduino codes of all prototypes can be accessed in [17].

4. Results

The prototypes were subjected to several tests in order to prove their operation in real situations, taking into account the cane application. Both control methods were tested, through full-state feedback (eq. (12)) with gain obtained by LQR and through Polynomial Pole Placement Techniques, and showed similar results, with the LQR option presenting smoother behaviour and the Pole Placement option showing a faster reaction. In Figure 10 it is possible to see the behaviour of the system, controlled by the two controllers, in a situation were the user walks at a normal speed, showing the smoother but slower response of the LQR option.

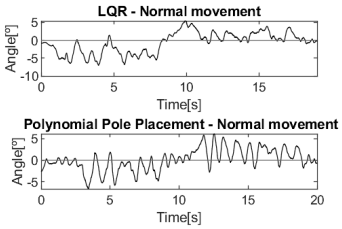

Figure 10: Comparison between the behaviours of the system with both controllers.

Overall, the LQR option showed a better behavior, even if with a slower reaction, being more predictable and comfortable. Because of this, only the system controlled through full-state feedback (eq. (12)) with gain obtained by LQR was analysed with all prototypes.

The difference between the behavior of the system controlled by polynomial pole placement techniques in the simulations of the section 2 and the behaviour in these real tests is justified by the fact that the system modeling is not perfect and the fact that, in the real system, there is a limit to the power that the actuators can manipulate, so a high increase in the gains leads only to saturation, not resulting in a better response by the system [10].

4.1. Bigger LEGO ® prototype

Figure 12 shows the angle of the bigger LEGO ® prototype during a 60-second test in which the cane was standing, with the user holding the rod without moving, as shown in Figure 11. The objective of the system is to maintain verticality while avoiding movements to the maximum. Throughout the test the variation of the angle never exceeds $\mp 1°$, therefore being very small variations, proving that the system can maintain its verticality. It should be noted that many of the variations that are observed result from the flexibility of the LEGO ® structure and small movements that are inevitably made by the user's hand, introducing some human error. The aluminium prototype, with its stronger structure, eliminates most of the jittery behaviour.

Although this prototype does not have the force sensors and, as such, it is not possible to calculate an angle and position reference, as explained in the section 2.2, the ability to reach angle references other than zero was tested. A reference was submitted to the system starting at $0°$, reducing to $-30°$ after 15 seconds, changing each 5 seconds for a new angle reference value. The values used were $-30°, -20°, -10°, -5°, 0°, 5°, 10°, 20°$ and $30°$, ending again at $0°$. Figure 13 corresponds to a moment during the test. Observing the be-

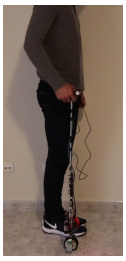

Figure 11: Test of the ability of the bigger LEGO ® prototype to maintain verticality when standing.

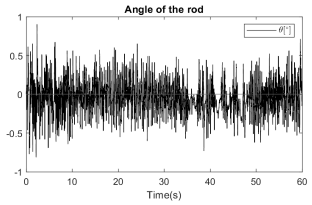

Figure 12: System response to the test of the bigger LEGO ® prototype's ability to maintain verticality when stopped.

havior of the system in Figure 14, it is possible to conclude that the system can always reach the desired reference, quickly and smoothly (important, considering the application that the cane will have). Again, it should be noted that, as in the previous case, many of the variations that are observed result from small movements that are inevitably made by the user's hand, and therefore there is a component of human error.

Figure 13: Test of the ability of the cane to reach the desired references.

The bigger LEGO ® prototype was tested for real use situations, following the user's movement, as seen in Figure 15. For this, the user carried out three tests, walking forward until covering a distance of $4.5m$, stopping for a brief moment and walking backwards to the starting point. In the first test, Figure 16, the user moved at a normal speed and with a normal gait, advancing with one foot always ahead of the previous one. In the second test, Figure 17, moved at a lower speed and joining the feet between each step, always advancing with the same foot, simulating the locomotion that an elderly person or someone with a injured

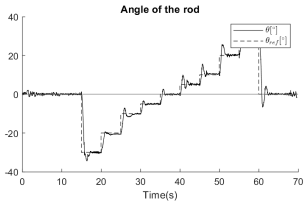

Figure 14: System response to the test of the cane's ability to reach the desired references.

lower limb would have. In the third test, Figure 18, moved at a higher speed, walking normally again, like in the first test.

The cane successfully kept up with the user's movement, staying close to vertical. The higher the speed, the bigger the force the user applies to the cane, which results in more intense angle variations, so the cane has more difficulty maintaining verticality in the case of faster movement, reaching up to 15°, while in the slower case it only peaked at 8°, remaining mostly below 2°.

In all cases, it is also possible to easily observe the user's steps. Each time a step is taken, the user's body moves and the arm pushes or pulls the cane, corresponding to the peaks of variation in its angle. When these variations are negative correspond to the forward movement of the user, which causes the cane to lean forward, and when they are positive correspond to the backwards movement.

Figure 15: Test of the ability of the cane to keep up with the normal movement of the user.

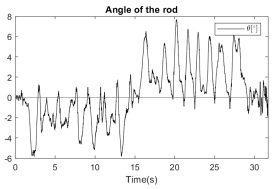

Figure 16: System response to the test of the cane's ability to keep up with the user's normal movement.

Testing the ability of the bigger LEGO ® prototype to support the user in the event of unbalance, helping to prevent a fall, the cane was placed in front of and behind the user, in two separate moments, and the user leaned towards the cane, supporting part of his weight, as shown in the Figure 19. It should be noted that due to the motors being used, the torque generated by the system is

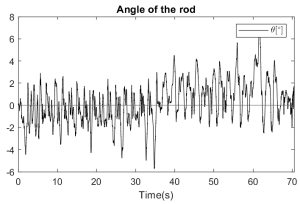

Figure 17: System response to the test of the cane's ability to keep up with the user's slow movement.

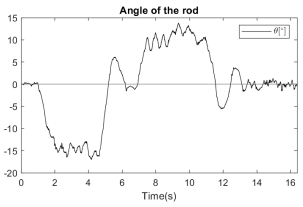

Figure 18: System response to the test of the cane's ability to keep up with the user's fast movement.

low, so the cane cannot withstand very high forces. However, it is possible to observe in Figure 20 that, even with these motors, the cane is able to support part of the user's weight, helping to regain balance and avoid falls. When the user is supported, there is a stabilization in the angle of the cane, which results from the force of the motors to counter the force that the user is applying to the cane, trying to bring the system back to verticality.

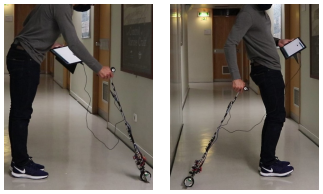

(a) Leaning forward. (b) Leaning back.

Figure 19: Test of the ability of the cane to hold its position and support the user in the event of an imminent fall.

All prototypes use the same two LEGO ® motors, being capable of producing $11Ncm$ of torque. In a test similar to Figure 20, the aluminium prototype was able to support $7N$ of force applied by the user at a 77°.

4.2. Aluminium prototype

The tests carried out on this prototype ensured the viability of the concept, having been carried out analyzes of the robot's behavior with users with and without reduced mobility capabilities.

In order to ensure the correct functioning of this prototype, tests were carried out with 7 individuals without mobility difficulties. In each test, the

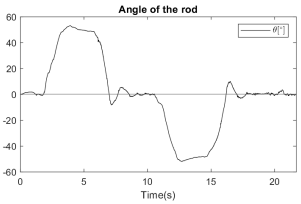

Figure 20: System response to the test of the cane's ability to hold its position and support the user in the event of an imminent fall.

user moved $4m$ forward, then turned around and advanced again to the starting point.

The results showed that the way one uses the cane varies a lot from person to person. Younger individuals kept the cane on their side and moved alongside it, keeping it fairly vertical. On the other hand, when the subjects were older, the cane was placed in front of the body, close to 20°, reporting that this was the position in which they felt most supported, behaving similarly with traditional walking canes.

The way users hold the cane also changed from case to case, but in all cases most of the force was applied over the back force sensor.

Two other tests were carried out, now on users with reduced mobility, the first being a case recovering locomotion capabilities and the second a case maintaining them, thus allowing to analyze the behavior of the system in the two main applications of the concept. The first user is recovering from a fracture, and thus showed some initial apprehension when seeing the cane, but then used it without any issue, only needing some support from another person in the beginning, while getting used. The second case, an user suffering from rheumatoid arthritis, showed immediate willingness to use the cane, and used it without any help. Both users complained that the support provided by the cane was not enough in some situations where they applied a higher force. In the end of the tests, the first user still preferred a traditional cane, while the second user preferred the robotic cane.

(a) User recovering from a fracture. (b) User with rheumatoid arthritis.

Figure 21: Tests with users with reduced mobility.

In both cases, users instinctively placed the cane in front of them, at a 20° angle, as what older subjects did in the tests with individuals without mobility difficulties. Observing the dynamics of a person standing, it is better understood why these users feel safer with the cane in front of them. Since the human body has only two points of contact with the ground, due to bipedia, it results in an unstable system if not properly controlled, requiring a third contact point to become stable in these cases. The success of the control depends on the agility, balance and cognitive fitness of each individual. As mentioned in [2] and [8], aging and a sedentary lifestyle lead to these capacities being reduced, worsening the control of the body to remain stable while standing and walking, thus increasing the risk of unbalance and falling.

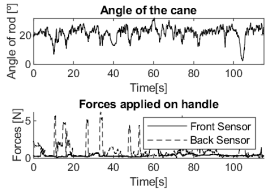

(a) User recovering from a fracture.

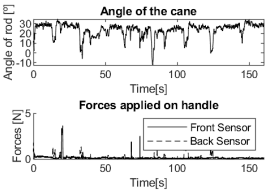

(b) User with rheumatoid arthritis.

Figure 22: System angle and forces applied on the tests with users with reduced mobility.

The balance of a standing person is based on the ability to maintain the projection of the center of mass on the ground within the polygon formed by the points in contact with the ground, that is, within the support polygon [24]. If the balance control is degraded due to age or other pathologies, the best solution is to counter this lack of control of the position of the center of mass by increasing the area of the polygon where it can be. In addition, the support polygon, this way, is extended in front of the user, which is the direction most propitious to unbalance since it corresponds to the direction of movement. In the Figure 23 the support polygons are represented when the individual does not use a cane, when he uses it at his side and when he uses it in front of him.

Thus, the reason for instinctively placing the cane in front of older users is justified. However, as younger users do not feel the need to increase the support polygon, they unconsciously place the cane beside them closer to vertical, thus helping to support part of the weight that would otherwise be placed on the lower limbs.

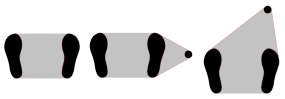

Figure 23: Support polygons in no cane (left), cane at side (middle) and cane at front (right) situations.

5. Conclusions

The model and prototype of the robotic cane developed in this study were proven to be a success. The behaviour of the system is very smooth and worked very well with the intended applications for the device. Its usage is very intuitive, making it natural for the user during their movement. Despite the limitations of the prototype built, its benefits in supporting the user throughout his movement, and the support of the user to regain balance in fall situations were proven with performance above expectations. The feedback from the test subjects and the medical team was very helpful and positive, thus confirming the viability of the concept.

In future work, the motor will be changed to a stronger motor, to improve the amount of support the cane can supply to the user. The control will be further adjusted to optimise the behaviour of the system for different situations, and an algorithm to calculate the reference from the force sensors of the handle will be created. The two controllers will also be merged, bringing the best of each one together to improve the overall behaviour of the system. Outdoor tests will also be conducted to verify the performance of the device in situations were the user has more space and freedom of movement.

Finally, one of the points to improve will also be the aesthetic component of the device, in order to become more attractive to users, encouraging its use.

Acknowledgements

This research is supported by Serviços Partilhados do Ministério da Saúde (SPMS) and Agrupamento de Centros de Saúde Loures-Odivelas (ACES Loures-Odivelas).

References

[1] Estatísticas Demográficas. 2020. accessed 21-December-2020.

[2] F. A. Barbieri and R. Vitório. *Locomotion and Posture in Older Adults: The Role of Aging and Movement Disorders.* 2017. accessed 28-October-2020.

[3] L. Burns. An extended framework for supply chain risk management: Incorporating the complexities of emerging industries and large-scale systems. *International Journal of Manufacturing Technology and Management*, 31(1-3):217–254, 2017.

[4] T. Fukuda, J. Huang, P. Di, and K. Sekiyama. Motion control and fall detection of intelligent cane robot. *Springer Tracts in Advanced Robotics*, 2015.

[5] A. Gmerek and E. Jezierski. Admittance control of a 1-DoF robotic arm actuated by BLDC motor. *2012 17th International Conference on Methods and Models in Automation and Robotics, MMAR 2012*, (August):633–638, 2012.

[6] S. L. Grondin and Q. Li. Intelligent control of a smart walker and its performance evaluation. *IEEE International Conference on Rehabilitation Robotics*, pages 1–6, 2013.

[7] P. Iglesias. Pole placement using polynomial methods. accessed 21-December-2020.

[8] M. Iosa, A. Fusco, G. Morone, and S. Paolucci. Development and decline of upright gait stability. *Frontiers in Aging Neuroscience*, 6(FEB):1–12, 2014.

[9] H. G. Jun, Y. Y. Chang, B. J. Dan, B. R. Jo, B. H. Min, H. Yang, W. K. Song, and J. Kim. Walking and sit-to-stand support system for elderly and disabled. *IEEE International Conference on Rehabilitation Robotics*, 2011.

[10] J. M. Lemos. *Controlo No Espaço De Estados*. IST PRESS, 1 edition, 2019.

[11] I. Lourtie. *Sinais e sistemas*. Escolar Editora, 2002.

[12] C. O. Lovejoy. Evolution of human walking. *Scientific American*, 259(5):118–125, 1988.

[13] L. N. Matheson, J. Verna, T. E. Dreisinger, S. Leggett, and J. Mayer. Age and gender normative data for lift capacity. *Work*, 49(2):257–269, 2014.

[14] R. Moreira, J. Alves, A. Matias, and C. Santos. Smart and Assistive Walker - ASBGo: Rehabilitation Robotics: A Smart-Walker to Assist Ataxic Patients. *Advances in experimental medicine and biology*, 1170:37–68, 2019.

[15] M. A. Naeem and S. F. Assal. Development of a 4-DOF cane robot to enhance walking activity of elderly. *Proceedings of the Institution of Mechanical Engineers, Part C: Journal of Mechanical Engineering Science*, 0(0):1–19, 2019.

[16] A. F. Neto, A. Elias, C. Cifuentes, C. Rodriguez, T. Bastos, and R. Carelli. Intelligent Assistive Robots. 106, 2015. accessed 19-February-2020.

[17] G. Neves. goncalomneves/RoboticCane. accessed 27-December-2020.

[18] G. Neves. Lightweight locomotion assistant for people - Technical Report. Technical report, 2020. accessed 27-December-2020.

[19] K. Ogata. *Engenharia de Controle Moderno*. Pearson, 5 edition, 2011.

[20] T. Ohnuma, G. Lee, and N. Y. Chong. Particle filter based feedback control of JAIST Active Robotic Walker. *Proceedings - IEEE International Workshop on Robot and Human Interactive Communication*, pages 264–269, 2011.

[21] A. J. Rentschler, R. Simpson, R. A. Cooper, and M. L. Boninger. Clinical evaluation of Guido robotic walker. *Journal of Rehabilitation Research and Development*, 45(9):1281–1294, 2008.

[22] R. D. Schraft, C. Schaeffer, and T. May. Care-O-botTM: The concept of a system for assisting elderly or disabled persons in home environments. *IECON Proceedings (Industrial Electronics Conference)*, 4:2476–2481, 1998.

[23] I. Shim and J. Yoon. A human robot interaction system RoJi. *IEEE/ASME International Conference on Advanced Intelligent Mechatronics, AIM*, 2:723–728, 2003.

[24] P. Vadakkepat and D. Goswami. Biped Locomotion: Stability, Analysis and Control. *International Journal on Smart Sensing and Intelligent Systems*, 1(1):187–207, 2008.

[25] P. Van Lam and Y. Fujimoto. Completed hardware design and controller of the robotic cane using the inverted pendulum for walking assistance. *IEEE International Symposium on Industrial Electronics*, pages 1935–1940, 2017.

[26] H. Wang, B. Sun, X. Wu, H. Wang, and Z. Tang. An intelligent cane walker robot based on force control. *2015 IEEE International Conference on Cyber Technology in Automation, Control and Intelligent Systems, IEEE-CYBER 2015*, pages 1333–1337, 2015.

[27] D. A. Winter. *Biomechanics and Motor Control of Human Movement: Fourth Edition*. 2009.